RETHINKING REWARD MODEL EVALUATION: ARE WE BARKING UP THE WRONG TREE?

Anonymous authors
Paper under double-blind review

ABSTRACT

Reward Models (RMs) are crucial for aligning language models with human preferences. Currently, the evaluation of RMs depends on measuring accuracy against a validation set of manually annotated preference data. Although this method is straightforward and widely adopted, the relationship between RM accuracy and downstream policy performance remains under-explored. In this work, we conduct experiments in a synthetic setting to investigate how differences in RM measured by accuracy translate into gaps in optimized policy performance. Our findings reveal that while there is a weak positive correlation between accuracy and downstream performance, policies optimized towards RMs with similar accuracy can exhibit quite different performance. Moreover, we discover that the way of measuring accuracy significantly impacts its ability to predict the final policy performance. Through the lens of the Regressional Goodhart effect, we recognize that accuracy, when used for measuring RM quality, can fail to fully capture the potential RM overoptimization. This underscores the inadequacy of relying solely on accuracy to reflect their impact on policy optimization.

1 INTRODUCTION

Reinforcement Learning from Human Feedback (RLHF) (Ibarz et al., 2018; Ouyang et al., 2022) has emerged as a prominent paradigm for aligning Large Language Models (Yang et al., 2024; Dubey et al., 2024). The reward model (Ng & Russell, 2000; Brown & Niekum, 2019; Palan et al., 2019) plays a crucial role in this process by substituting human preferences for model optimization. However, building an RM that fully captures human preferences is highly challenging (Armstrong & Mindermann, 2019; Skalse & Abate, 2023; Lambert et al., 2023). Therefore, the RM can be an imperfect proxy for ideal preferences and cause downstream performance deterioration when optimized against it, known as reward model overoptimization (Gao et al., 2022). This phenomenon, as a result of Goodhart's law (Karwowski et al., 2023), presents a critical challenge to the RLHF.

The difficulty of constructing an ideal RM require a reliable evaluation to capture potential negative impacts in policy optimization. To date, common practice for evaluating the RM includes directly assessing the optimized policy (Hendrycks et al., 2021; Li et al., 2023) and computing accuracy on a fixed dataset (Lambert et al., 2024). While the former approach serves as a final metric, it is constrained by the cost of optimization and cannot distinguish whether undesirable behaviors stem from the policy optimization process or the reward learning process. The latter approach remains the question of whether such evaluation accurately predicts the performance of the optimized policy.

In this work, we systematically investigate the effectiveness of using accuracy in predicting downstream performance. Essentially, the accuracy metric measures the difference between two reward functions, referred to as **RM error**. In practice, the accuracy quantifies the error between the learned reward model and the empirical human rewards. The RM error can lead to potential performance loss between the policies optimized for the proxy RM and the golden reward function. Specifically, we define this performance gap as **Policy Regret**. Therefore, the goal of RM evaluation is to predict policy regret through RM error, as depicted in Figure 1.

To investigate how differences in RM measured by accuracy translate into gaps in optimized policy performance, we design a synthetic experiment framework. Due to the inaccessibility of human reward functions, we employ synthetic RM as the golden reward function in our experiments. To effectively collect golden-proxy RM pairs for analysis, we create N different RMs, designating one

RM as the golden model and the others as proxy models each time. Based on the above framework, we decompose the issue concerning RM evaluation into three research questions (RQ):

RQ1: Does the RM error measured by accuracy correlate with the policy regret? We examine the correlation between the accuracy and the policy regret on the widely adopted RewardBench dataset(Lambert et al., 2024). We employ optimization algorithms, i.e., best-of-n sampling and policy gradient-based reinforcement learning, for investigation. Our findings reveal a weak positive correlation between the measured accuracy and the policy regret. However, we observe that policies optimized towards reward models within a similar accuracy range can have quite different regrets.

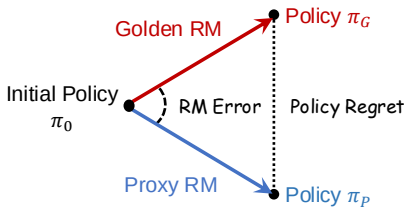

Figure 1: Translation from RM error to policy regret.

RQ2: How to better measure RM error for policy regret prediction? While we present a positive correlation between the accuracy and the policy regret, there remains room for further enhancement. This naturally raises the question of how to better quantify RM error to achieve a stronger correlation. We begin by investigating the influence of prompt and response distributions. Specifically, we observe that the prompt difference between the RM test dataset and the downstream test dataset will potentially decrease the correlation between the accuracy and the policy regret. Regarding response distribution, we find that the rank of responses evaluated by the golden RM impacts correlation more significantly than the model from which they are sampled. Furthermore, we propose a simple yet effective strategy to enhance correlation: increasing the number of responses per prompt in the test dataset. We validate this approach under constraints of equal sample size and annotation budget, finding that metrics based on more responses achieve a higher correlation with policy regret.

RQ3: What's the relationship between RM error and Policy Regret? The translation from RM error to policy regret stems from the overoptimization of the reward model. Specifically, optimizing toward an imperfect proxy RM leads to a deterioration in downstream performance. Therefore, to predict the policy regret, the quantified RM error should be able to reflect the potential overoptimization. In this work, we derive the expected relationship between the accuracy and the degree of reward overoptimization under the assumptions of Regressional Goodhart's effect (Manheim & Garrabrant, 2019) and normal distributions of both reward score and noise. However, our findings indicate that RMs with similar accuracy can behave quite differently in terms of overoptimization. This indicates accuracy alone can be an inadequate metric for predicting the downstream performance.

In summary, our work provides deeper understanding into the relationship between RM error and policy regret. This offers valuable insights for both reward model training and the development of a more robust RLHF algorithm. Our results also highlight the need for a more rigorous benchmark in reward model evaluation and the development of advanced RM assessment tools.

2 Preliminary

Let $\mathcal{X}$ be the set of prompts, and $\mathcal{Y}_\mathcal{X}$ be the set of possible responses. A policy π is a language model that generates responses y to the prompt x at probability $\pi(y|x)$. The golden reward function assesses the response and gives a score based on their quality $r^* : \mathcal{X} \times \mathcal{Y}_\mathcal{X} \to \mathbb{R}$. In practice, the golden reward function r represents the complicated human preference and is generally inaccessible. Instead, a reward model r learned from preference data serves as the proxy of the golden reward function r^*. Then policy π is optimized to maximize the expectation of the reward given by r:

$$\pi = \max_{\pi} \mathbb{E}_{x \in \mathcal{X}, y \sim \pi(\cdot|x)}[r(x, y)] \tag{1}$$

This results in a sub-optimal policy π rather than the ideal policy π^* that directly maximizes the reward given by the golden reward function r^*.

The workflow of Reinforcement Learning from Human Feedback (RLHF) can be represented as:

- $\mathcal{A}_{RM}(D_{RM}^{train}) \to r$: Learn a proxy RM r on the preference dataset D_{RM}^{train} by algorithm $\mathcal{A}_{RM}$.
- $\mathcal{M}(r, r^*|D_{RM}^{test}) \to d_r$: Evaluate the RM error between proxy reward model r and golden reward function r^* by metric $\mathcal{M}$ on the test dataset D_{RM}^{test}.

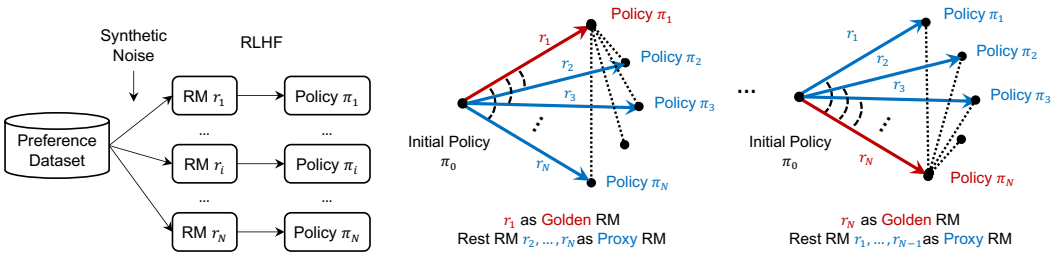

(a) Synthetic pipeline of Reinforcement Learning from Human Feedback.

(b) Proxy-golden RM pairs collection for evaluating the correlation between the RM error and policy regret.

Figure 2: Overall experiment framework.

- $\mathcal{A}_{RL}(\pi_0, r|D_{RL}^{train}) \rightarrow \pi$: Optimize the initial policy π_0 and get policy π that maximizes the expectation of reward given by the proxy RM r by the algorithm $\mathcal{A}_{RL}$.
- $\mathcal{M}'(\pi, \pi^*|D_{RL}^{test}) \rightarrow d_\pi$: Measure the regret between the policy π and the policy π^* that optimized directly towards r^* by metric $\mathcal{M}'$ on the test dataset D_{RL}^{test}.

In this work, we essentially focus on the relationship between the error of reward model d_r and the regret of policy d_π, which translates our issue into: **How should we measure the error d_r so as to reach high correlation with the policy regret d_π**? Various factors introduced in the RLHF process can potentially influence this relationship. To systematically investigate their impact, we focus on several key factors while keeping other variables fixed. The test dataset D_{RM}^{test} on which the reward model r is evaluated; The metric $\mathcal{M}$ used to evaluate the error between the reward models; The test dataset D_{RL}^{test} on which the final policy π is evaluated.

One challenge in conducting the investigation is the inaccessibility of the golden reward function representing human preferences. To address this difficulty, we follow the previous practice (Gao et al., 2022; 2024) of utilizing another reward model to act as the golden reward function.

Another challenge is to effectively collect the proxy-golden RM pairs for evaluating the correlation between the RM error and policy regret. We implement this by constructing $N = 10$ different reward models r_i by randomly flipping α_i of the pairs in the training dataset[1] D_{RM}^{train}. Then N policies π_i will be optimized towards the corresponding reward model r_i. This pipeline is demonstrated in Figure 2a. This operation will form $N \times (N-1)$ golden-proxy RM pairs. As shown in Figure 2b, these pair collections can then be used for computing correlation by letting one reward model as the golden reward function and the remaining reward models as proxy reward models.

Building on prior works that formally define policy regret in the context of general Markov Decision Processes (MDPs) (Karwowski et al., 2023; Fluri et al., 2024), we adapt the concept within the framework of RLHF. Given that the KL divergence between a policy π and the initial policy π_0 is $KL(\pi||\pi_0) = \lambda$, the regret with respect to a golden reward function r^* is defined as:

$$Reg_{r^*} = \frac{\max_{KL(\pi'||\pi_0)<\lambda} J_{r^*}(\pi') - J_{r^*}(\pi)}{\max_{KL(\pi'||\pi_0)<\lambda} J_{r^*}(\pi') - \min_{KL(\pi'||\pi_0)<\lambda} J_{r^*}(\pi')} \tag{2}$$

Here, the function $J_{r^*}(\pi) = \mathbb{E}_{y\sim\pi(\cdot|x)}[r^*(x, y)]$ represents the expected reward given the policy π and the golden reward function r^*. This value reflects the ratio of the maximum reward gain a policy can achieve to the actual reward gain obtained, considering the constraint of KL divergence.

However, this definition is hard to compute due to the inaccessibility of the optimal policy and the difficulty of controlling KL divergence λ. Therefore, we propose **Normalised Drop Ratio (NDR)** as a computable estimation as follows:

$$\mathcal{M}'_{NDR}(\pi, \pi^*) = \frac{J_{r^*}(\pi) - J_{r^*}(\pi_0)}{J_{r^*}(\pi^*) - J_{r^*}(\pi_0)} \tag{3}$$

[1]We constructed the data such that if a training set has α_i of its labels flipped and another has α_j flipped, then $|\alpha_i - \alpha_j|\%$ of the labels are inconsistent between the two sets. See Appendix 8.1 for dataset details.

where the policies π and π^* are achieved by optimizing initial policy π_0 against the golden reward function r^* and the proxy RM r with exactly the same hyperparameters. This metric quantifies the performance deterioration resulting from optimizing against a proxy RM r instead of the golden reward function r^*. It also accounts for variations due to different scales among different RMs.

The data from the RewardBench (Lambert et al., 2024) are used to construct the test datasets D_{RM}^{test} and D_{RL}^{test}. All RMs are initialized from the Llama-3-instruct-8B model (AI@Meta, 2024) and finetuned by minimizing the negative log-likelihood loss with regularization term (Hou et al., 2024):

$$\mathcal{L}_{RM} = -\mathbb{E}_{(x,y_w,y_l)\sim D_{RM}^{train}}[\log(\sigma(r(x,y_w) - r(x,y_l)))] - \mathbb{E}_{(x,y)\sim D_{RM}^{train}}[r(x,y)^2] \quad (4)$$

We adopt best-of-n sampling (BoN) and PPO (Schulman et al., 2017) as the algorithm A_{RL} to optimize the initial policy π_0, which is also the Llama-3-instruct-8B model. For the best-of-n sampling, the reward model r picks the response with the highest reward from n candidates. For the PPO algorithm, we follow (Gao et al., 2022) and set the KL penalty in all experiments to be 0.

3 Does the RM error measured by accuracy correlate with the policy regret?

Current research typically assesses reward model errors by computing accuracy on a fixed test set. Although widely used, it remains unclear whether the accuracy correlates with policy regret. In this section, we evaluate the accuracy and policy regret using the RewardBench (Lambert et al., 2024) dataset. We perform deduplication on the prompts, leaving 2,733 distinct prompts.

Finding 1: *RM evaluation accuracy is positively related to policy regret, but even with similar RM accuracy, policies can exhibit different levels of regret.*

We first investigate the correlation between accuracy and policy regret. Original RewardBench prompts and responses are used to measure accuracy, and the prompts are used for downstream optimization. We calculate the correlations between RM error, measured by accuracy, and policy regret, measured by NDR, in Table 1. As presented in Figure 3a and Figure 3b, there is a positive relationship between accuracy and policy regret. However, trends illustrate that policy regret can vary considerably even within similar accuracy ranges. Lastly, we observe that accuracy generally correlates more strongly with regret in BoN than in PPO. This is expected, as BoN is a more localized and stable optimization algorithm, making it more predictable by reward model error.

Table 1: The correlation between the accuracy (**Acc.**) and the policy regret under BoN and PPO measured by typical correlation coefficients and Mean Reciprocal Rank (**MRR**). MRR is calculated by averaging the reciprocal ranks of policies optimized by the RM with the highest accuracy.

Error / Regret		Relevance			
		Kendall τ corr.	Pearson corr.	Spearman corr.	MRR
Acc.	BoN	0.6561	0.7520	0.7533	0.6333
Acc.	PPO	0.4654	0.6395	0.6102	0.5167

4 How to better measure RM error for policy regret prediction?

In the previous section, we examine the positive correlation between accuracy and policy regret. However, there appears to be room for enhancing this correlation, which leads us to the question: how to better quantify the RM error? In this section, we first investigate the influence of prompt and response distribution. Moreover, we explore a straightforward yet effective strategy, i.e., extending responses per prompt. Finally, we validate it under different constraints.

Finding 2: *The rank of responses affects the correlation between accuracy and regret more than the response sampling models.*

In the previous experiment, we used the original responses in RewardBench for validation, which were sampled from different models. This naturally raises the question: **Is it possible to achieve**

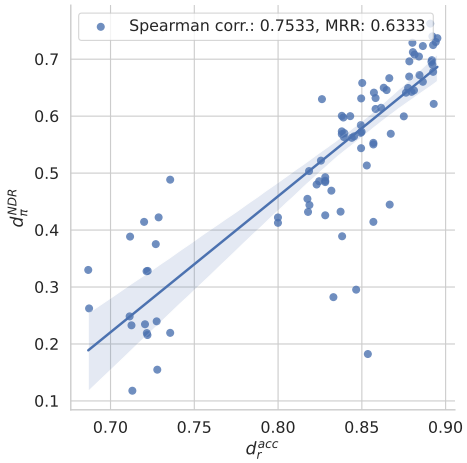

(a) Trend between accuracy d_r^{acc} and the policy regret d_π^{NDR} under BoN setting.

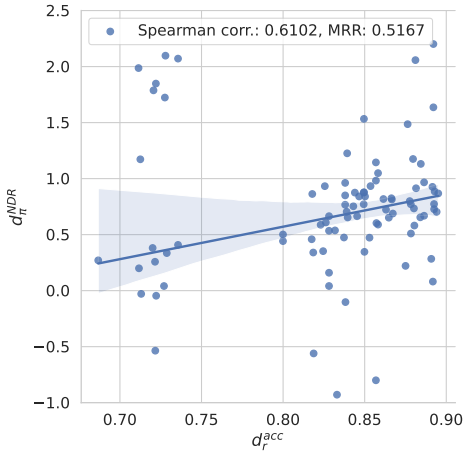

(b) Trend between the accuracy d_r^{acc} and the policy regret d_π^{NDR} under PPO setting.

Figure 3: Trend between the accuracy and policy regret measured by the normalised drop ratio.

Table 2: The correlation between policy regret and accuracy on datasets with responses sampled from different models. The **Origin** represents the result on the RewardBench dataset. The highest results are highlighted in **bold**. The model used for downstream optimization is suffixed with *.

Model	BoN		PPO	
	Spearman corr.	MRR	Spearman corr.	MRR
Mistral-7B	0.680±0.042	0.579±0.079	0.580±0.037	0.573±0.073
Llama3-8B*	0.644±0.038	0.598±0.080	**0.648±0.047**	0.551±0.061
Qwen2-7B	0.680±0.030	0.529±0.074	0.603±0.039	**0.599±0.060**
Vicuna-7b	0.703±0.035	**0.658±0.075**	0.527±0.036	0.517±0.068
Origin	**0.753**	0.633	0.610	0.517

a higher correlation by sampling responses exclusively from the model used for downstream optimization? To examine this question, we construct multiple test datasets, each containing responses exclusively sampled from a single downstream model.. We then evaluate the correlation between policy regret and computed accuracy. As shown in Table 2, this approach does not consistently improve upon the original RewardBench dataset. This result suggests that sampling responses from the model used for optimization may not be necessary to achieve a strong correlation.

While it seems unnecessary to sample from models used for optimization, we observe varying correlations in datasets constructed with responses by different models. This indicates that other factors, such as **the rank of chosen and rejected samples**, may be at play. To examine this assumption, we prepare multiple responses for all prompts. Each time, we sort the responses by golden rewards given by one RM, and divide them into bins. We then randomly sample accepted and rejected responses from different bins to construct test datasets with responses of varying ranks. The accuracy on these test datasets is used to assess the correlation with policy regrets. As demonstrated in Figure 4a and Figure 4b, different trends emerged for BoN and PPO. For BoN, test datasets with chosen samples from mid-rank bins and rejected samples from lower-rank bins exhibited higher correlations. In contrast, for PPO, datasets with chosen samples from higher-rank bins and rejected samples from mid-rank bins showed a stronger correlation. This distinction likely stems from the characteristics of the two optimization algorithms. With PPO, the policy is optimized more aggressively, causing responses to rank higher under the golden RM, making the consistency between the proxy RM and the golden RM on high-reward samples more critical. Conversely, for BoN, where the degree of policy optimization is less intense, consistency on mid-reward samples can be more instructive.

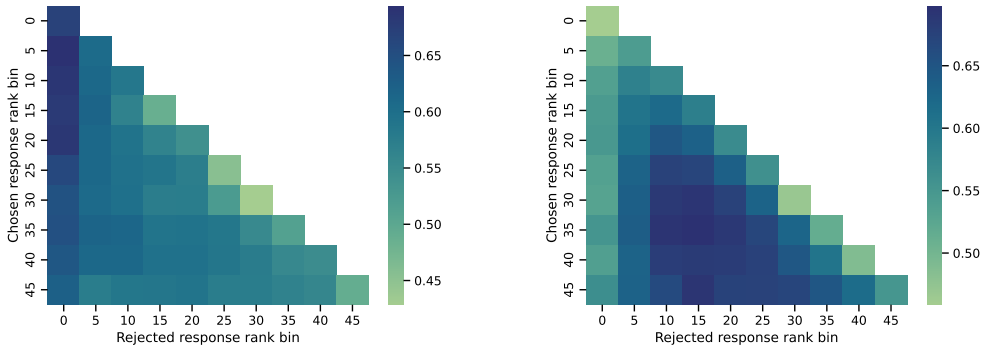

(a) The correlation trend on BoN.

(b) The correlation trend on PPO.

Figure 4: The correlation between policy regret and accuracy on datasets constructed from responses. Each grid on the x and y axes represents a sampled bin, with the values below indicating the corresponding rank. For example, the 5 on the y-axis indicates that the chosen responses are sampled from those ranked between 5 and 10.

Table 3: The correlation between policy regret and accuracy on the test dataset composed of prompts from different categories evaluated by the Spearman coefficient. The highest result in each column is **bolded**, and the highest in each row is underlined.

Regret		Accuracy				
		Chat	ChatHard	Code	Math	Safety
BoN	Chat	**0.529±0.082**	0.682±0.058	0.573±0.050	0.557±0.052	0.657±0.044
	ChatHard	0.493±0.089	0.682±0.053	0.583±0.038	0.538±0.066	0.655±0.051
	Code	0.504±0.095	0.634±0.059	**0.717±0.043**	0.456±0.060	0.646±0.053
	Math	0.288±0.121	0.343±0.080	0.244±0.048	**0.610±0.058**	0.282±0.059
	Safety	0.515±0.093	**0.705±0.057**	0.521±0.047	0.497±0.067	**0.687±0.049**
PPO	Chat	0.349±0.105	0.500±0.086	0.441±0.054	0.192±0.083	**0.611±0.061**
	ChatHard	0.314±0.115	0.484±0.083	0.434±0.057	0.202±0.087	0.576±0.073
	Code	0.384±0.092	0.450±0.080	**0.527±0.051**	**0.371±0.060**	0.459±0.053
	Math	0.185±0.091	0.275±0.064	0.238±0.050	0.145±0.057	0.313±0.054
	Safety	**0.359±0.118**	**0.521±0.062**	0.442±0.061	0.332±0.069	0.533±0.053

Finding 3: *The prompt difference between the RM test dataset and downstream test dataset can weaken the accuracy-regret correlation.*

The previous experiments assume that the RM and RL test datasets consisted of the same prompts, which may not be true in practice. To investigate **the influence of prompt category**, wWe split the test dataset based on the prompt categories determined by the original classifications in RewardBench. We evaluate accuracy and regret in each category and demonstrate the results in Table 3. We find that accuracies in each category align more closely with regret in the corresponding category under the BoN setting. However, this relationship is not present in the PPO setting. This may be because different types of prompts influence each other during PPO optimization.

To further investigate **the influence of prompt semantics**, we randomly rewrite some prompts in the original test dataset, creating new test datasets with prompts different from the downstream dataset. We ask GPT-4o (OpenAI, 2024) to perform two different strategies on these prompts, as detailed in Appendix 8.2. One strategy alters the expression without changing the meaning, and the other generates a new prompt within the same category. As shown in Figure 5, we find that the correlation is less affected by paraphrasing under BoN. However, the correlation measured by the Spearman coefficient on PPO continuously weakens as we paraphrase a larger ratio of prompts.

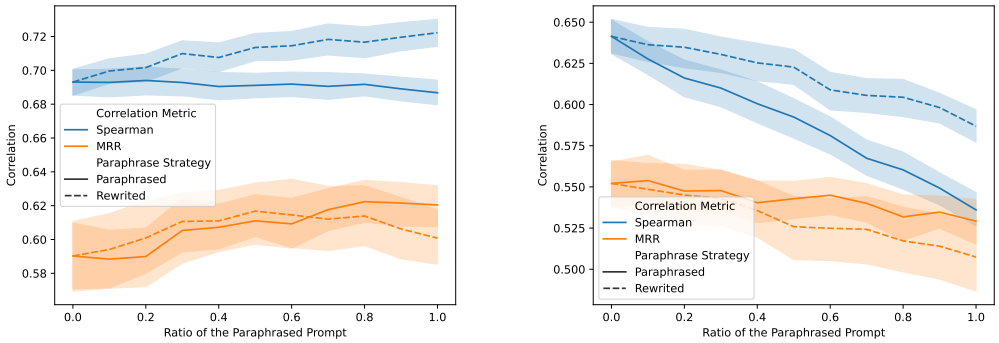

(a) The correlation trend on BoN.

(b) The correlation trend on PPO.

Figure 5: The correlation between policy regret and accuracy on datasets with different ratios of paraphrased prompts evaluated by the Spearman coefficient and MRR. Different line styles are used to represent datasets paraphrased by different strategies.

Table 4: The correlation between different metrics and policy regret. The **Accuracy-pair** stands for the baseline that only samples two responses per prompt and computes the accuracy. Metrics that require an absolute score for each response are suffixed with *.

Metrics	BoN		PPO	
	Spearman corr.	MRR	Spearman corr.	MRR
Pearson corr.*	0.663±0.012	0.657±0.040	0.685±0.016	0.545±0.020
Spearman corr.	0.664±0.015	0.664±0.046	0.680±0.019	0.552±0.030
Kendall τ corr.	0.665±0.016	**0.667±0.042**	0.686±0.019	0.558±0.035
Accuracy	0.656±0.015	0.648±0.036	0.671±0.018	0.554±0.025
Bo5*	0.666±0.020	0.663±0.058	0.670±0.024	0.543±0.032
ECE	0.173±0.016	0.364±0.027	0.063±0.014	0.382±0.022
MRR	0.650±0.018	0.646±0.054	0.675±0.022	0.565±0.042
NDCG	0.655±0.032	0.614±0.071	0.658±0.039	0.562±0.053
ξ corr.	**0.677±0.026**	0.649±0.051	**0.688±0.026**	**0.583±0.047**
Accuracy-pair	0.635±0.039	0.586±0.080	0.642±0.047	0.567±0.082

Finding 4: *Increasing the number of responses per prompt can enhance the correlation between measured RM error and policy regret.*

We first examine the strategy of response expansion per prompt by preparing 5 responses per prompt and **employing various metrics**. The details about the computation of these metrics can be found in Appendix 8.8. These metrics include common correlation measures, as well as metrics adapted from Information Retrieval. We also explored other metrics for comparison, e.g., expected calibration error and Bo5. Note that some metrics require absolute scoring of responses, which may be inaccessible in practice. As shown in Table 4, metrics evaluated on the dataset with more responses consistently achieve higher correlations in comparison to the accuracy on the dataset with two responses per prompt. Moreover, the ξ correlation (Chatterjee, 2020) generally demonstrated the best performance. The ECE metric, despite its relative commonness, does not show a significant correlation with regret.

Although measuring more responses per prompt yields a higher correlation, it can be unfair without controlling for the total number of samples (prompt-response pairs) in the test dataset. Thus, we further explore the question of whether we should increase the number of responses or prompts while maintaining a constant sample size. We fix the sample size in the test dataset while varying the number of responses. As shown in Figure 6a and Figure 6b, it is generally more effective to increase the number of responses rather than the number of prompts. However, this advantage

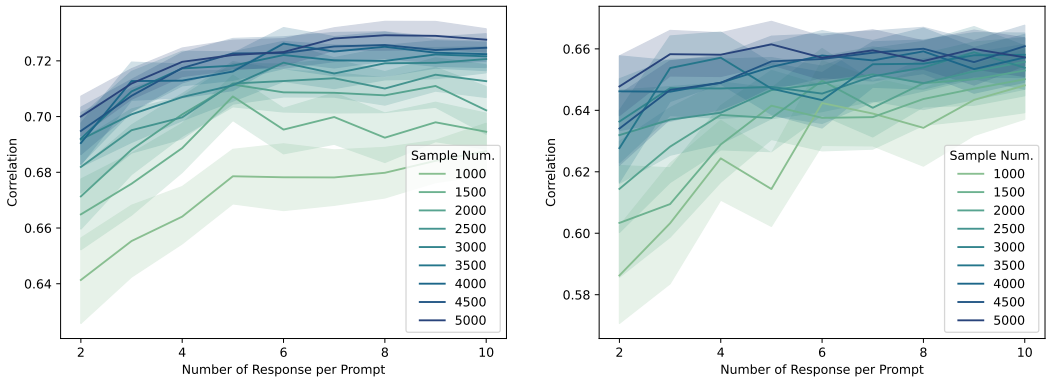

(a) The correlation trend on BoN.

(b) The correlation trend on PPO.

Figure 6: The Spearman coefficient between accuracy and policy regret with test datasets having the same number of samples but varying numbers of responses per prompt.

decreases with the growing sample size, possibly due to reaching an upper bound in the correlation between regret and measured accuracy.

The annotation cost can be another important factor since building a test dataset with more than two responses can be tricky. To explore this factor, we further examine the question that **should we increase responses or prompts under a constant annotation budget**. To conduct the experiment, we consider the noise in the annotation process. Among various probability ranking models (Critchlow et al., 1991), we adopt the most commonly used one, i.e., the Bradley-Terry model (Bradley & Terry, 1952). Given a prompt x and two responses y_i and y_j, the probability that y_i is preferred to y_j is computed by:

$$P(y_i \succ y_j|x) = \frac{1}{1 + e^{(r_j - r_i)/\beta}} \tag{5}$$

where r_i and r_j is the golden reward score given to the response y_i and y_j in our case. The parameter β, which can be seen as an indicator of the annotation quality, is set to 0.5. We evaluate the annotation cost by measuring the number of pairwise comparisons. This setting fits the Bradley-Terry model and is also commonly adopted in real-world practice. The annotation process is stimulated by performing a sorting algorithm based on pair-wise comparison. The final results are presented in Figures 7a and 7b. We find that under the BoN setting, including more responses is more beneficial with the same annotation budget. However, with a limited annotation budget, the benefits quickly diminish as the number of responses grows. Additionally, in the PPO setting, increasing the number of responses does not yield significant advantages.

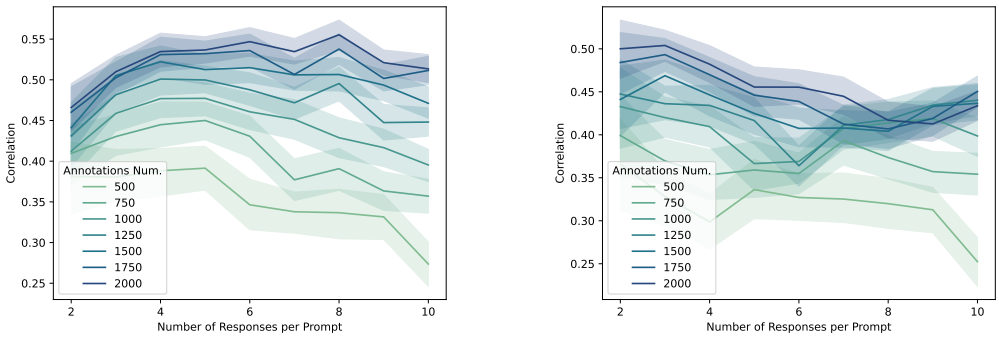

(a) The correlation trend on BoN.

(b) The correlation trend on PPO.

Figure 7: The Spearman coefficient between policy regret and accuracy on test datasets with the same annotation budget but varying the number of responses per prompt.

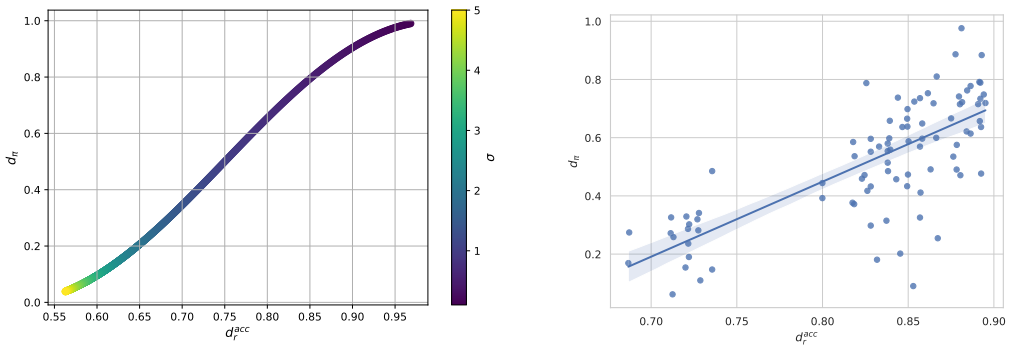

(a) Expected trend of accuracy d_r^{acc} and the degree of overoptimization d_π by varying the noise σ.

(b) The trend of the accuracy d_r^{acc} and the estimated degree of overoptimization d_π under BoN.

Figure 8: Trends between the accuracy d_r^{acc} and the degree of overoptimization d_π.

5 What's the relationship between RM error and Policy Regret?

In this section, we investigate the relationship between RM error and policy regret. The translation from RM error to the policy regret can be seen as the result of the reward model overoptimization. Therefore, to accurately predict policy regret, the quantified RM error should be able to reveal the potential overoptimization. We first theoretically explore this issue. Then we empirically examine the relationship and analyze the observed optimization dynamics.

Finding 5: *Accuracy alone can be insufficient to capture the potential RM overoptimization.*

Goodhart's Law (Goodhart, 1984) is the main cause for the translation from RM error to policy regret. It states that optimizing a less effective metric rather than the golden metric leads to system failure. Such a phenomenon is also commonly termed reward model overoptimization (Gao et al., 2022) under the context of RLHF. Among the various kinds of Goodhart's effect that lead to reward model overoptimization, the Regressional Goodhart effect (Manheim & Garrabrant, 2019) is the most fundamental and unavoidable. It occurs when the proxy reward model r is essentially the golden reward function r^* mixed with some independent noise z, namely:

$$r = r^* + z \tag{6}$$

Assuming that only the Regressional Goodhart effect occurs and both the reward score and noise are normally distributed, i.e. $r^* \sim \mathcal{N}(0, \sigma_r^2)$ and $z \sim \mathcal{N}(0, \sigma^2)$, the relationship between accuracy d_r^{acc} and the degree of overoptimization d_π [2] can be expressed by the following parametric equations:

$$\begin{aligned} d_r^{acc} &= 1 - \int_{x=0}^{+\infty} \frac{1}{\sigma_r \sqrt{\pi}} e^{-\frac{x^2}{4\sigma_r^2}} \Phi\left(-\frac{x}{\sqrt{2}\sigma}\right) dx \\ d_\pi &= \frac{\sigma_r^2}{\sigma_r^2 + \sigma^2} \end{aligned} \tag{7}$$

where Φ denotes the cumulative distribution function of the standard normal distribution.. The equation is too complex to be solved analytically, so we resort to a numerical solution. We plot the expected relationship between accuracy and the degree of overoptimization in Figure 8a.

However, the trend under the BoN setting, as plotted in Figure 8b, reveals outliers beyond the expected relationship. These discrepancies may stem from other forms of Goodhart's effects (Manheim & Garrabrant, 2019) beyond the Regressional type. Figure 9 illustrates the optimization dynamics when using different golden RMs and optimizing towards various proxy RMs. We observe distinct overoptimization phenomena for golden-proxy RM pairs that have similar accuracy levels. In Figure 9a, there is nearly no drop in golden reward scores as the KL divergence increases, indicating that the Regressional Goodhart's effect is dominant in this case. In contrast, Figure 9b shows

[2] The definition of d_π and detailed derivation are provided in Appendix 8.9.

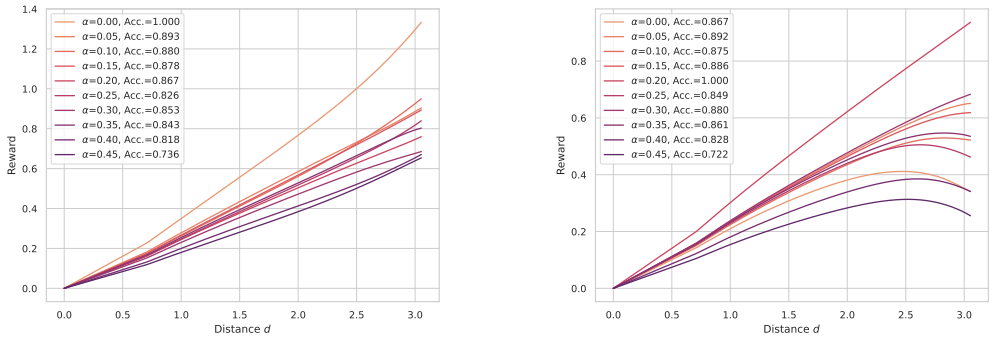

(a) RM with $\alpha = 0$ as golden reward model.

(b) RM with $\alpha = 0.15$ as golden reward model.

Figure 9: Overoptimization trends under BoN setting. The change of golden reward score when optimizing towards different proxy RMs are plotted. The distance d is computed as $\sqrt{D_{KL}(\pi||\pi_0)}$ (Bai et al., 2022), where the KL divergence of best-of-n sampling can be computed by $\log n - \frac{n-1}{n}$ (Hilton, 2023). The rewards are computed by an unbiased estimator (Nakano et al., 2022).

a noticeable decline in golden reward scores across nearly all proxy RMs, suggesting the influence of more complex Goodhart's effects. These differences suggest that solely relying on accuracy may be insufficient to predict potential overoptimization.

6 Related Works

Reinforcement Learning from Human Feedback (RLHF) (Bai et al., 2022; Ouyang et al., 2022; Stiennon et al., 2022) has been a common strategy for the alignment of Large Language Models (Yang et al., 2024; Dubey et al., 2024), in which the reward model plays a crucial role. However, this methodology faces several challenges (Casper et al., 2023; Lang et al., 2024; Armstrong & Mindermann, 2019; Skalse et al., 2022), such as reward model overoptimization (Gao et al., 2022; Lehman et al., 2019), where optimizing policy towards proxy reward model may lead to the ground truth performance deterioration. This phenomenon, as a special case of reward hacking (Krakovna, 2020), can seen as the result of Goodhart's law (Goodhart, 1984; Zhuang & Hadfield-Menell, 2021).

The RM as an imperfect proxy of the golden preference necessitates the evaluation of whether the reward model accurately captures the real preference (Michaud et al., 2020; Russell & Santos, 2019). Many works consider the measurements to predict the potential consequence due to the difference of reward functions (Ng et al., 1999; Skalse et al., 2023). (Gleave et al., 2021; Skalse et al., 2024) propose the metric quantify the difference between the reward functions and induce regret bounds for optimal policies. However, some works (Zhuang & Hadfield-Menell, 2021; Fluri et al., 2024) propose negative visions of optimization towards imperfect proxy RMs. These works assume the accessibility of the golden reward function, which can be false under the RLHF setting. The common practice under RLHF is to compute accuracy on a fixed preference dataset (Lambert et al., 2024), which remains the question about theoretical or empirical validation of performance prediction.

7 Conclusion

Our study highlights that although there is a weak positive correlation between accuracy and policy performance, RMs with similar accuracy can result in varying policy outcomes. Moreover, the method used to measure accuracy significantly impacts prediction performance. Finally, we find that accuracy alone may not fully reflect the phenomenon of overoptimization. Overall, we suggest a more cautious attitude about RM performance as indicated by accuracy and emphasize the importance of developing more sophisticated RM evaluation techniques..

REFERENCES

AI@Meta. Llama 3 model card. 2024. URL https://github.com/meta-llama/llama3/blob/main/MODEL_CARD.md.

Argilla. Capybara-dpo 7k binarized dataset. https://huggingface.co/datasets/argilla/distilabel-capybara-dpo-7k-binarized, 2024.

Stuart Armstrong and Sören Mindermann. Occam's razor is insufficient to infer the preferences of irrational agents, 2019. URL https://arxiv.org/abs/1712.05812.

Yuntao Bai, Andy Jones, Kamal Ndousse, Amanda Askell, Anna Chen, Nova DasSarma, Dawn Drain, Stanislav Fort, Deep Ganguli, Tom Henighan, Nicholas Joseph, Saurav Kadavath, Jackson Kernion, Tom Conerly, Sheer El-Showk, Nelson Elhage, Zac Hatfield-Dodds, Danny Hernandez, Tristan Hume, Scott Johnston, Shauna Kravec, Liane Lovitt, Neel Nanda, Catherine Olsson, Dario Amodei, Tom Brown, Jack Clark, Sam McCandlish, Chris Olah, Ben Mann, and Jared Kaplan. Training a helpful and harmless assistant with reinforcement learning from human feedback, 2022. URL https://arxiv.org/abs/2204.05862.

Ralph Allan Bradley and Milton E. Terry. Rank analysis of incomplete block designs: I. the method of paired comparisons. *Biometrika*, 39(3/4):324, 1952. doi: 10.2307/2334029. URL https://doi.org/10.2307/2334029.

Daniel S. Brown and Scott Niekum. Deep bayesian reward learning from preferences, 2019. URL https://arxiv.org/abs/1912.04472.

Stephen Casper, Xander Davies, Claudia Shi, Thomas Krendl Gilbert, Jérémy Scheurer, Javier Rando, Rachel Freedman, Tomasz Korbak, David Lindner, Pedro Freire, Tony Wang, Samuel Marks, Charbel-Raphaël Segerie, Micah Carroll, Andi Peng, Phillip Christoffersen, Mehul Damani, Stewart Slocum, Usman Anwar, Anand Siththaranjan, Max Nadeau, Eric J. Michaud, Jacob Pfau, Dmitrii Krasheninnikov, Xin Chen, Lauro Langosco, Peter Hase, Erdem Bıyık, Anca Dragan, David Krueger, Dorsa Sadigh, and Dylan Hadfield-Menell. Open problems and fundamental limitations of reinforcement learning from human feedback, 2023. URL https://arxiv.org/abs/2307.15217.

Sourav Chatterjee. A new coefficient of correlation, 2020. URL https://arxiv.org/abs/1909.10140.

Douglas E Critchlow, Michael A Fligner, and Joseph S Verducci. Probability models on rankings. *Journal of Mathematical Psychology*, 35(3):294–318, September 1991. ISSN 00222496. doi: 10.1016/0022-2496(91)90050-4.

Ganqu Cui, Lifan Yuan, Ning Ding, Guanming Yao, Wei Zhu, Yuan Ni, Guotong Xie, Zhiyuan Liu, and Maosong Sun. Ultrafeedback: Boosting language models with high-quality feedback, 2023.

Luigi Daniele and Suphavadeeprasit. Amplify-instruct: Synthetically generated diverse multi-turn conversations for efficient llm training. *arXiv preprint arXiv:(coming soon)*, 2023. URL https://huggingface.co/datasets/LDJnr/Capybara.

Abhimanyu Dubey, Abhinav Jauhri, Abhinav Pandey, Abhishek Kadian, Ahmad Al-Dahle, Aiesha Letman, Akhil Mathur, Alan Schelten, Amy Yang, Angela Fan, Anirudh Goyal, Anthony Hartshorn, Aobo Yang, Archi Mitra, Archie Sravankumar, and other. The llama 3 herd of models, 2024. URL https://arxiv.org/abs/2407.21783.

Lukas Fluri, Leon Lang, Alessandro Abate, Patrick Forré, David Krueger, and Joar Skalse. The perils of optimizing learned reward functions: Low training error does not guarantee low regret, 2024. URL https://arxiv.org/abs/2406.15753.

Deep Ganguli, Liane Lovitt, Jackson Kernion, Amanda Askell, Yuntao Bai, Saurav Kadavath, Ben Mann, Ethan Perez, Nicholas Schiefer, Kamal Ndousse, Andy Jones, Sam Bowman, Anna Chen, Tom Conerly, Nova DasSarma, Dawn Drain, Nelson Elhage, Sheer El-Showk, Stanislav Fort, Zac Hatfield-Dodds, Tom Henighan, Danny Hernandez, Tristan Hume, Josh Jacobson, Scott Johnston, Shauna Kravec, Catherine Olsson, Sam Ringer, Eli Tran-Johnson, Dario Amodei, Tom Brown,

Nicholas Joseph, Sam McCandlish, Chris Olah, Jared Kaplan, and Jack Clark. Red teaming language models to reduce harms: Methods, scaling behaviors, and lessons learned, 2022. URL https://arxiv.org/abs/2209.07858.

Leo Gao, John Schulman, and Jacob Hilton. Scaling laws for reward model overoptimization, 2022. URL https://arxiv.org/abs/2210.10760.

Yang Gao, Dana Alon, and Donald Metzler. Impact of preference noise on the alignment performance of generative language models, 2024. URL https://arxiv.org/abs/2404.09824.

Adam Gleave, Michael Dennis, Shane Legg, Stuart Russell, and Jan Leike. Quantifying differences in reward functions, 2021. URL https://arxiv.org/abs/2006.13900.

C. A. E. Goodhart. *Problems of Monetary Management: The UK Experience*, pp. 91–121. Macmillan Education UK, London, 1984. ISBN 978-1-349-17295-5. doi: 10.1007/978-1-349-17295-5_4. URL https://doi.org/10.1007/978-1-349-17295-5_4.

Dan Hendrycks, Collin Burns, Steven Basart, Andy Zou, Mantas Mazeika, Dawn Song, and Jacob Steinhardt. Measuring massive multitask language understanding, 2021. URL https://arxiv.org/abs/2009.03300.

Jacob Hilton. KL divergence of max-of-n. December 2023.

Zhenyu Hou, Yilin Niu, Zhengxiao Du, Xiaohan Zhang, Xiao Liu, Aohan Zeng, Qinkai Zheng, Minlie Huang, Hongning Wang, Jie Tang, and Yuxiao Dong. Chatglm-rlhf: Practices of aligning large language models with human feedback, 2024. URL https://arxiv.org/abs/2404.00934.

Jian Hu, Xibin Wu, Weixun Wang, Xianyu, Dehao Zhang, and Yu Cao. Openrlhf: An easy-to-use, scalable and high-performance rlhf framework. *arXiv preprint arXiv:2405.11143*, 2024.

Borja Ibarz, Jan Leike, Tobias Pohlen, Geoffrey Irving, Shane Legg, and Dario Amodei. Reward learning from human preferences and demonstrations in atari, 2018. URL https://arxiv.org/abs/1811.06521.

Intel. Orca dpo pairs dataset. https://huggingface.co/datasets/Intel/orca_dpo_pairs, 2023. Available on Hugging Face Datasets.

Jiaming Ji, Donghai Hong, Borong Zhang, Boyuan Chen, Josef Dai, Boren Zheng, Tianyi Qiu, Boxun Li, and Yaodong Yang. Pku-saferlhf: A safety alignment preference dataset for llama family models, 2024. URL https://arxiv.org/abs/2406.15513.

Jacek Karwowski, Oliver Hayman, Xingjian Bai, Klaus Kiendlhofer, Charlie Griffin, and Joar Skalse. Goodhart's law in reinforcement learning, 2023. URL https://arxiv.org/abs/2310.09144.

Victoria Krakovna. Specification gaming: The flip side of ai ingenuity, April 2020. URL https://deepmind.google/discover/blog/specification-gaming-the-flip-side-of-ai-ingenuity/.

Nathan Lambert, Thomas Krendl Gilbert, and Tom Zick. The history and risks of reinforcement learning and human feedback, 2023. URL https://arxiv.org/abs/2310.13595.

Nathan Lambert, Valentina Pyatkin, Jacob Morrison, LJ Miranda, Bill Yuchen Lin, Khyathi Chandu, Nouha Dziri, Sachin Kumar, Tom Zick, Yejin Choi, Noah A. Smith, and Hannaneh Hajishirzi. Rewardbench: Evaluating reward models for language modeling, 2024. URL https://arxiv.org/abs/2403.13787.

Leon Lang, Davis Foote, Stuart Russell, Anca Dragan, Erik Jenner, and Scott Emmons. When your ais deceive you: Challenges of partial observability in reinforcement learning from human feedback, 2024. URL https://arxiv.org/abs/2402.17747.

Joel Lehman, Jeff Clune, Dusan Misevic, Christoph Adami, Lee Altenberg, Julie Beaulieu, Peter J. Bentley, Samuel Bernard, Guillaume Beslon, David M. Bryson, Patryk Chrabaszcz, Nick Cheney, Antoine Cully, Stephane Doncieux, Fred C. Dyer, Kai Olav Ellefsen, Robert Feldt, Stephan Fischer, Stephanie Forrest, Antoine Frénoy, Christian Gagné, Leni Le Goff, Laura M. Grabowski, Babak Hodjat, Frank Hutter, Laurent Keller, Carole Knibbe, Peter Krcah, Richard E. Lenski, Hod Lipson, Robert MacCurdy, Carlos Maestre, Risto Miikkulainen, Sara Mitri, David E. Moriarty, Jean-Baptiste Mouret, Anh Nguyen, Charles Ofria, Marc Parizeau, David Parsons, Robert T. Pennock, William F. Punch, Thomas S. Ray, Marc Schoenauer, Eric Shulte, Karl Sims, Kenneth O. Stanley, François Taddei, Danesh Tarapore, Simon Thibault, Westley Weimer, Richard Watson, and Jason Yosinski. The surprising creativity of digital evolution: A collection of anecdotes from the evolutionary computation and artificial life research communities, 2019. URL https://arxiv.org/abs/1803.03453.

Xuechen Li, Tianyi Zhang, Yann Dubois, Rohan Taori, Ishaan Gulrajani, Carlos Guestrin, Percy Liang, and Tatsunori B. Hashimoto. Alpacaeval: An automatic evaluator of instruction-following models. https://github.com/tatsu-lab/alpaca_eval, 5 2023.

Wing Lian, Bleys Goodson, Eugene Pentland, Austin Cook, Chanvichet Vong, and "Teknium". Openorca: An open dataset of gpt augmented flan reasoning traces. https://https://huggingface.co/Open-Orca/OpenOrca, 2023.

David Manheim and Scott Garrabrant. Categorizing variants of goodhart's law, 2019. URL https://arxiv.org/abs/1803.04585.

Eric J. Michaud, Adam Gleave, and Stuart Russell. Understanding learned reward functions, 2020. URL https://arxiv.org/abs/2012.05862.

Reiichiro Nakano, Jacob Hilton, Suchir Balaji, Jeff Wu, Long Ouyang, Christina Kim, Christopher Hesse, Shantanu Jain, Vineet Kosaraju, William Saunders, Xu Jiang, Karl Cobbe, Tyna Eloundou, Gretchen Krueger, Kevin Button, Matthew Knight, Benjamin Chess, and John Schulman. Webgpt: Browser-assisted question-answering with human feedback, 2022. URL https://arxiv.org/abs/2112.09332.

Andrew Y. Ng and Stuart J. Russell. Algorithms for inverse reinforcement learning. In *Proceedings of the Seventeenth International Conference on Machine Learning*, ICML '00, pp. 663–670, San Francisco, CA, USA, 2000. Morgan Kaufmann Publishers Inc. ISBN 1558607072.

Andrew Y. Ng, Daishi Harada, and Stuart J. Russell. Policy invariance under reward transformations: Theory and application to reward shaping. In *Proceedings of the Sixteenth International Conference on Machine Learning*, ICML '99, pp. 278–287, San Francisco, CA, USA, 1999. Morgan Kaufmann Publishers Inc. ISBN 1558606122.

OpenAI. Gpt-4o system card. https://openai.com/research/gpt-4o-system-card.pdf, 2024.

Long Ouyang, Jeff Wu, Xu Jiang, Diogo Almeida, Carroll L. Wainwright, Pamela Mishkin, Chong Zhang, Sandhini Agarwal, Katarina Slama, Alex Ray, John Schulman, Jacob Hilton, Fraser Kelton, Luke Miller, Maddie Simens, Amanda Askell, Peter Welinder, Paul Christiano, Jan Leike, and Ryan Lowe. Training language models to follow instructions with human feedback, 2022. URL https://arxiv.org/abs/2203.02155.

Malayandi Palan, Nicholas C. Landolfi, Gleb Shevchuk, and Dorsa Sadigh. Learning reward functions by integrating human demonstrations and preferences, 2019. URL https://arxiv.org/abs/1906.08928.

Jacob Russell and Eugene Santos. Explaining reward functions in markov decision processes. In *The Thirty-Second International FLAIRS Conference*, 2019.

John Schulman, Filip Wolski, Prafulla Dhariwal, Alec Radford, and Oleg Klimov. Proximal policy optimization algorithms, 2017. URL https://arxiv.org/abs/1707.06347.

Joar Skalse and Alessandro Abate. Misspecification in inverse reinforcement learning, 2023. URL https://arxiv.org/abs/2212.03201.

Joar Skalse, Nikolaus H. R. Howe, Dmitrii Krasheninnikov, and David Krueger. Defining and characterizing reward hacking, 2022. URL https://arxiv.org/abs/2209.13085.

Joar Skalse, Matthew Farrugia-Roberts, Stuart Russell, Alessandro Abate, and Adam Gleave. Invariance in policy optimisation and partial identifiability in reward learning, 2023. URL https://arxiv.org/abs/2203.07475.

Joar Skalse, Lucy Farnik, Sumeet Ramesh Motwani, Erik Jenner, Adam Gleave, and Alessandro Abate. Starc: A general framework for quantifying differences between reward functions, 2024. URL https://arxiv.org/abs/2309.15257.

Nisan Stiennon, Long Ouyang, Jeff Wu, Daniel M. Ziegler, Ryan Lowe, Chelsea Voss, Alec Radford, Dario Amodei, and Paul Christiano. Learning to summarize from human feedback, 2022. URL https://arxiv.org/abs/2009.01325.

Qwen Team. Qwen2.5: A party of foundation models, September 2024. URL https://qwenlm.github.io/blog/qwen2.5/.

An Yang, Baosong Yang, Binyuan Hui, Bo Zheng, Bowen Yu, Chang Zhou, Chengpeng Li, Chengyuan Li, Dayiheng Liu, Fei Huang, Guanting Dong, Haoran Wei, Huan Lin, Jialong Tang, Jialin Wang, Jian Yang, Jianhong Tu, Jianwei Zhang, Jianxin Ma, Jianxin Yang, Jin Xu, Jingren Zhou, Jinze Bai, Jinzheng He, Junyang Lin, Kai Dang, Keming Lu, Keqin Chen, Kexin Yang, Mei Li, Mingfeng Xue, Na Ni, Pei Zhang, Peng Wang, Ru Peng, Rui Men, Ruize Gao, Runji Lin, Shijie Wang, Shuai Bai, Sinan Tan, Tianhang Zhu, Tianhao Li, Tianyu Liu, Wenbin Ge, Xiaodong Deng, Xiaohuan Zhou, Xingzhang Ren, Xinyu Zhang, Xipin Wei, Xuancheng Ren, Xuejing Liu, Yang Fan, Yang Yao, Yichang Zhang, Yu Wan, Yunfei Chu, Yuqiong Liu, Zeyu Cui, Zhenru Zhang, Zhifang Guo, and Zhihao Fan. Qwen2 technical report, 2024. URL https://arxiv.org/abs/2407.10671.

Lianmin Zheng, Wei-Lin Chiang, Ying Sheng, Siyuan Zhuang, Zhanghao Wu, Yonghao Zhuang, Zi Lin, Zhuohan Li, Dacheng Li, Eric. P Xing, Hao Zhang, Joseph E. Gonzalez, and Ion Stoica. Judging llm-as-a-judge with mt-bench and chatbot arena, 2023.

Banghua Zhu, Evan Frick, Tianhao Wu, Hanlin Zhu, and Jiantao Jiao. Starling-7b: Improving llm helpfulness & harmlessness with rlaif, November 2023.

Simon Zhuang and Dylan Hadfield-Menell. Consequences of misaligned ai, 2021. URL https://arxiv.org/abs/2102.03896.

8 Appendix

8.1 Dataset Construction

We build up a RM training dataset by mixing the following open-sourced datasets:

- **Nectar** (Zhu et al., 2023), a high-quality 7-wise comparison dataset generated by GPT-4 ranking.
- **Capybara-7K-binarized** (Argilla, 2024), a binarized prefernce dataset built with distilabel atop the **Capybara** (Daniele & Suphavadeeprasit, 2023).
- **Orca-pairs** (Intel, 2023), a dataset contains 12k examples from OpenOrca dataset (Lian et al., 2023).
- **UltraFeedback** (Cui et al., 2023), a large-scale, fine-grained, diverse preference dataset.
- **PKU-SafeRLHF** (Ji et al., 2024), a high-quality dataset consisting of 83.4K preference entries, which is annotated across two dimensions: harmlessness and helpfulness.
- **MTBench-human** (Zheng et al., 2023), a dataset contains 3.3K expert-level pairwise human preferences for model responses generated by 6 models in response to 80 MT-bench questions.
- **Chatbot-arena** (Zheng et al., 2023), a dataset contains 33K cleaned conversations with pairwise human preferences. Responses generated by 6 models in response to 80 MT-bench questions.

Table 5: The prompt used for paraphrase strategy.

Now you should play the role of prompt engineer. Your task is to paraphrase the prompt into a new prompt. If the origin prompt is a safety-related prompt, paraphrase it into a new safe prompt. When outputting, only provide the paraphrased prompt and nothing else. >> Input Prompt: {prompt} >> Output:

Table 6: The prompt used for rewrite strategy.

Now you should play the role of prompt engineer. You should generate a new prompt of the same category with an input prompt. If the origin prompt is a safety-related prompt, paraphrase it into a new safe prompt. When outputting, only provide the generated prompt and nothing else. >> Input Prompt: {prompt} >> Output:

- **HH-RLHF** (Bai et al., 2022; Ganguli et al., 2022), a dataset contains human preference data about helpfulness and harmlessness.

We retain only single-turn dialogue data, deduplicating based on prompt string matching. Next, we filtered out excessively long samples and balanced the proportion of positive and negative sample lengths. Ultimately, we retained 112400 preference data samples, with 7052 set aside as a validation set for reward model training.

8.2 Paraphrase Prompts

We employed two strategies for rewriting prompts: one that alters expression without changing semantics, and another that rewrites the prompt into a similar but related prompt. The prompt in Table 5 is used for the paraphrase strategy, and the prompt in Table 6 is used for the rewrite strategy.

8.3 Relationship between Golden-Proxy Pairs

In this section, we present the relationship between golden-proxy pairs from our experiments. First, we illustrate the accuracy between golden RMs and proxy RMs in Figure 10. As shown, the image is symmetrical, and generally, as the data noise decreases, the accuracy between each golden-proxy pair increases. Next, we display the relationship of the NDR metric between proxy-golden pairs under BoN and PPO optimization. These figures do not exhibit obvious symmetry, and there are more extreme values under PPO optimization.

8.4 Correlation between Accuracy and Downstream Performance

In real-world scenarios, various factors can lead to discrepancies between proxy RMs and golden RMs. In the main experiments, we primarily considered noise in the training dataset. In this section, we explore two other common scenarios: 1) differences in model architecture between the proxy RM and the golden RM, and 2) differences in training data. For the first scenario, we train RMs using various Qwen2.5 Team (2024) series pretrain and instruct models, ranging from 0.5 to 72 billion parameters. For the second scenario, we randomly divide the training into $N = 10$ parts, using the first i parts to train the i-th RM. We then measure the correlation between the accuracy of these two types of RMs and the policy regret optimized through BoN, as shown in Figure 12a

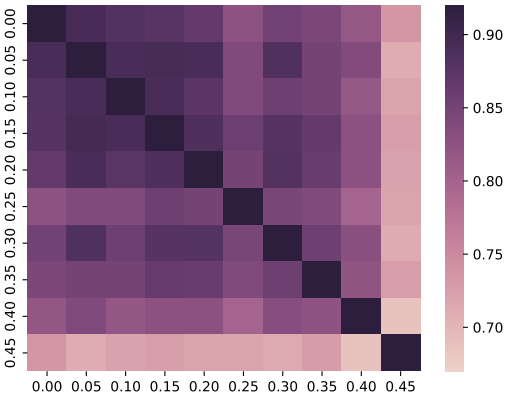

Figure 10: The accuracy between golden and proxy RMs across varying noise levels in training data.

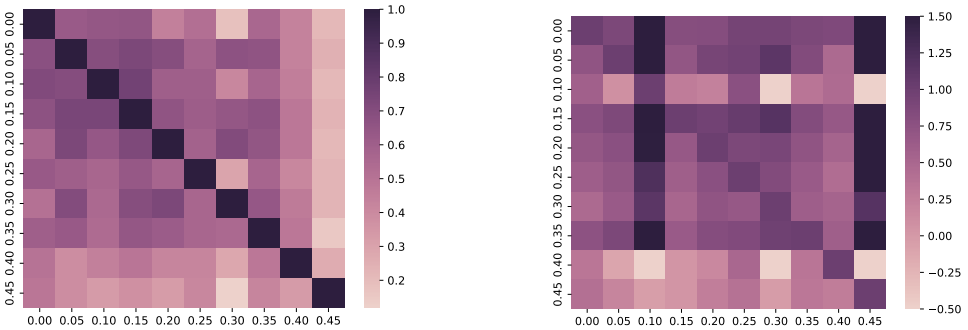

(a) The NDR metric under BoN setting.

(b) The NDR metric under PPO setting.

Figure 11: The NDR metrics between proxy-golden pairs under different settings.

and Figure 12b. The results indicate that the correlation for RMs trained on different datasets is significantly lower than for those trained on the same dataset with different models, possibly due to their high similarity indicated by accuracy.

Beyond synthetic environments, we also explore the relationship between RM metrics and downstream task performance in more realistic scenarios. We assess the accuracy of various open-source RMs on RewardBench Lambert et al. (2024) and examine their correlation with downstream tasks using MT-Bench Zheng et al. (2023), evaluated with GPT-4o. For evaluating downstream task performance, we optimize LLaMA-3-Instruct (AI@Meta, 2024) using Best-of-32. The results, shown in Figure 13, indicate a positive correlation between RewardBench metrics and MT-Bench scores. However, RMs with similar accuracy can lead to fluctuating downstream performance.

8.5 Influence of KL Penalty

In the main experiment, the KL penalty was set to 0. However, there remains the question of whether a larger KL penalty might increase the correlation with PPO. In this section, we examine the correlation between accuracy and PPO NDR using the same RMs from the main experiment but with varying KL penalties. The results in Table 7 indicate that appropriately increasing the KL penalty enhance the Spearman correlation while reduces the MRR. When the KL penalty becomes too large, the Spearman correlation also decreases. We believe that with a smaller KL penalty, the PPO optimization process becomes more localized and stable, thereby strengthening the predictive correlation

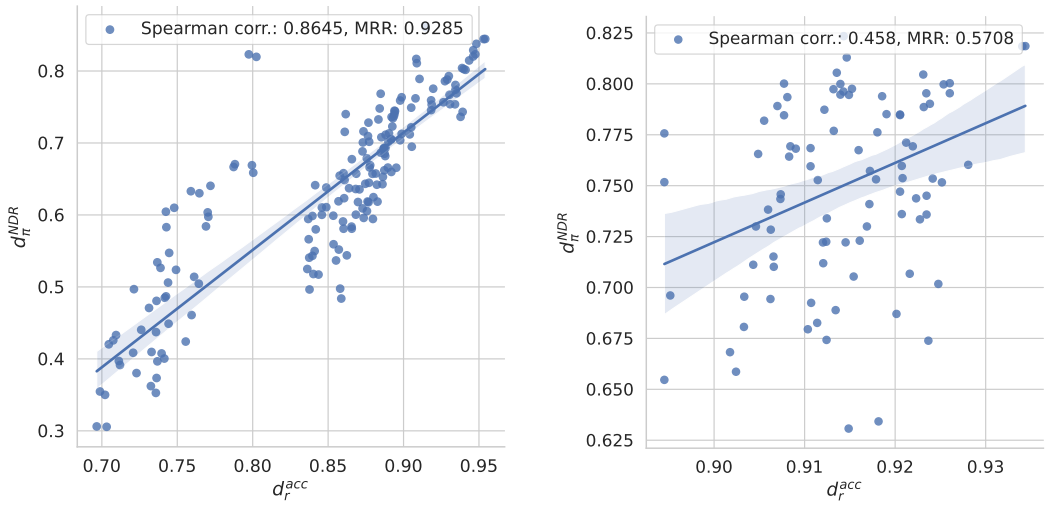

(a) The correlation trend under model scaling setting.

(b) The correlation trend under dataset split setting.

Figure 12: The correlation between accuracy and policy regret for RMs of different settings.

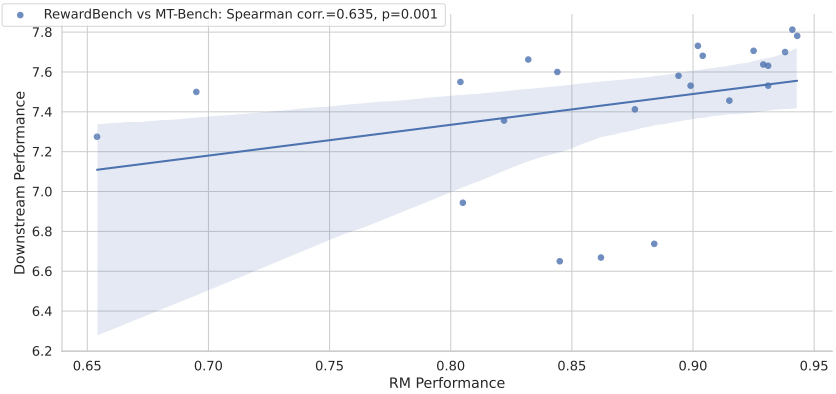

Figure 13: The correlation between RewardBench metric and MT-Bench score.

of RM error. However, the presence of the KL penalty limits the consistent increase of the expected reward, reducing the likelihood that a policy optimized with a best proxy RM result in the best policy. Once the KL penalty exceeds a certain threshold, the KL reward begins to dominate in the later optimization stages, hindering further growth of the expected reward. This increases the influence of uncertainty in PPO optimization, leading to a decline in correlation. We also experiment with a larger KL penalty (KL Penalty = 0.5), finding that its effects could even cause training to collapse.

Table 7: The correlation between the accuracy and the policy regret with different KL penalties.

KL Penalty	Relevance			
	Kendall τ corr.	Pearson corr.	Spearman corr.	MRR
0.00	0.3980	0.6981	0.4840	0.5158
0.01	0.3743	0.5345	0.5011	0.4950
0.05	0.5487	0.7461	0.6692	0.3960
0.10	0.4925	0.6267	0.6265	0.3750

8.6 INFLUENCE OF SAMPLE SIZE

In Figure 6, we observe that increasing the number of responses improves correlation. However, it remains question of whether further expanding the sample size will continue to enhance correlation or not. Therefore, in this section, we examine how correlation changes with larger sample sizes. Since the original RewardBench contains only 2,733 different prompts, increasing the sample size to over 5,500 with just two responses per prompt can be infeasible. For sample sizes greater than 5,500, we only assess the correlation in cases with more than two responses per prompt, adjusting the number of responses accordingly for even larger sizes. From the result depicted in Figure 14, we find that further expanding the sample size does not significantly enhance correlation; rather, it gradually approaches an upper limit.

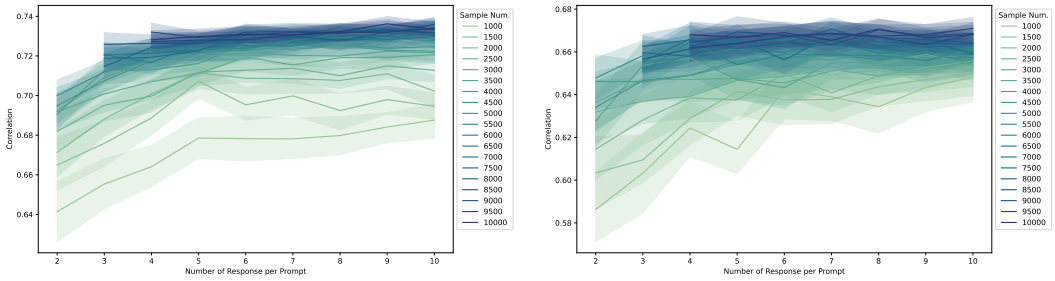

(a) The correlation trend on BoN.

(b) The correlation trend on PPO.

Figure 14: The correlation between accuracy and policy regret on test datasets with the same number of samples but varying numbers of responses per prompt assessed by the Spearman coefficient.

8.7 INFLUENCE OF DOWNSTREAM MODEL ON EXPANDING RESPONSE

In previous experiments, we use LLaMA-3-8b-Instruct as the downstream model and found that increasing the number of responses improved correlation with downstream performance. However, it remains questions of whether this effect holds with different downstream models. In this section, we use Qwen-2.5-7B-Instruct (Team, 2024) as the downstream model to test if increasing the number of responses still enhances correlation. As shown in the Figure 15, increasing the number of responses continues to be beneficial strategy with a different downstream policy.

8.8 REWARD ERROR METRICS

Given a prompt x and $N = 5$ different responses $Y = [y_1, ..., y_N]$, their corresponding reward scores and ranks are represented as $r(Y)$ and $R(Y)$. Since each prompt has multiple annotated responses, many ranking evaluation metrics can be applied to our setting. Finally, we averaged the correlation metrics across all prompts to obtain the results presented in the Table 4.

Pearson corr. Pearson correlation coefficient can be computed as follows:

$$\rho_{r(Y),r^*(Y)} = \frac{cov\left(r(Y), r^*(Y)\right)}{\sigma_{r(Y)}\sigma_{r^*(Y)}} \tag{8}$$

where cov is the covariance, $\sigma_{r(Y)}$ is the standard deviation of the proxy rewards given to the responses $r(Y)$ and $\sigma_{r^*(Y)}$ is the standard deviation of the golden rewards given to the responses $r^*(Y)$. The formula of $cov\left(r(Y), r^*(Y)\right)$ can be writed as:

$$cov\left(r(Y), r^*(Y)\right) = \mathbb{E}\left[(r(Y) - \mu_{r(Y)})(r^*(Y) - \mu_{r^*(Y)})\right] \tag{9}$$

Where $\mu_{r(Y)}$ and $\mu_r^*(Y)$ are the mean of the proxy rewards and golden rewards given to the responses, respectively. The final metric is the average of the coefficient of each prompt.

Spearman corr. Spearman's rank correlation coefficient follows the basically same formula as the Pearson correlation coefficient, only with the reward scores replaced by the ranks:

$$s_{R(Y),R^*(Y)} = \frac{cov\left(R(Y), R^*(Y)\right)}{\sigma_{R(Y)}\sigma_{R^*(Y)}} \tag{10}$$

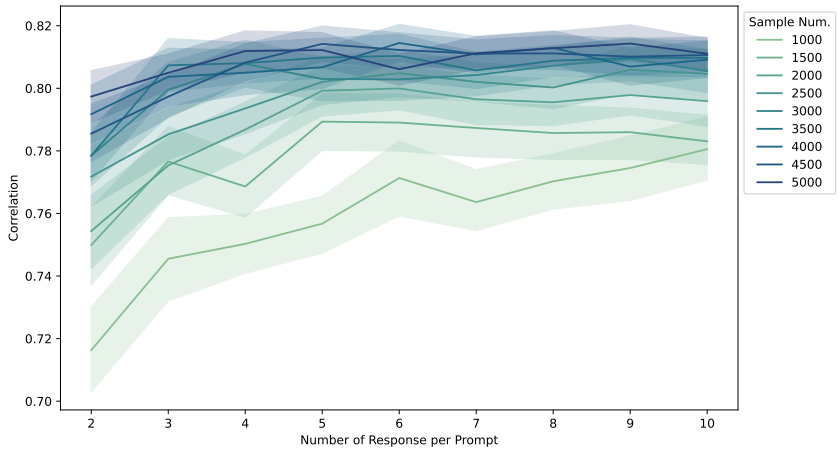

Figure 15: The Spearman coefficient between accuracy and policy regret with test datasets having the same number of samples but varying numbers of responses per prompt.

Kendall τ corr. Kendall rank correlation coefficient is computed as follows:

$$\tau_{R(Y),R^*(Y)} = \frac{n_c - n_d}{N(N-1)/2} \tag{11}$$

where n_c and n_d stands for the number of concordant and disconcordant pair between $R(Y)$ and $R^*(Y)$, respectively. The concordant pair (y_i, y_j) means that their rank satisfy $(R(Y_i) - R(Y_j))(R^*(Y_i) - R^*(Y_j)) > 0$. In practice, we employ τ_B which handles the ties for the rare case that some responses get the same reward scores. The final metric is the average of the coefficient of each prompt.

Accuracy The accuracy metrics are mostly the same as in the typical case that there are two responses per response. The main difference is that if there are N responses per response, we can then form C_N^2 different pairs for comparison.

Bo5 The best-of-5 metric can be seen as a special case of **NDR** for $N = 5$, which computes:

$$\frac{r^*\left(\arg\max_{y_i}\left[r(Y)\right]\right) - \mu_{r^*(Y)}}{\max\left[r^*(Y)\right] - \mu_{r^*(Y)}} \tag{12}$$

This metric represents the improvement in reward values obtained using the proxy reward score compared to those achievable with the original golden reward model. The final metric is the average of the coefficient of each prompt.

ECE Expected Calibration Error (ECE) is calculated by averaging the absolute differences between predicted probabilities and observed frequencies, typically across a set of bins partitioning the prediction space:

$$ECE = \sum_{m=1}^{M} \frac{|B_m|}{n} |acc(B_m) - conf(B_m)| \tag{13}$$

where B represents the bins that split pairs by reward margins and M stands for the number of bins. acc is the accuracy of pairs in each bin. $conf$ computes the expected accuracy inferred from reward score margins by the Bradley-Terry Model (Bradley & Terry, 1952). Expected calibration error indicate the alignment of reward models' confidence. We follow the same strategy for form preference pairs as in the **Accuracy**.

MRR Mean reciprocal rank is a traditional Information Retrieval metric that can be transported to our setting smoothly. We first define reciprocal rank as the golden rank of the response that receives

the highest reward score.[3]. Then we take the average overall prompts:

$$MRR = \mathbb{E}_{x \in \mathcal{X}} \left[\frac{1}{R^* \left[\arg\max_{y_i} \left[R(Y) \right] \right]} \right] \tag{14}$$

NDCG Normalized discounted cumulative gain is another typical Information Retrieval metric that is transported here. This computes compute:

$$NDCG = \frac{\sum_{i=1}^{N} (R^*(Y_i) - 1) / \log_2(N - R(Y_i) + 1)}{\sum_{i=1}^{N} (R^*(Y_i) - 1) / \log_2(N - R^*(Y_i) + 1)} \tag{15}$$

The main difference from the typical usage in the field of Information Retrieval is that we replace relevance score rel_i with the golden rank $R(Y_i)$. These metrics can be seen as a smooth version of **MRR**. The final metric is the average of the coefficient of each prompt.

ξ **corr.** ξ correlation coefficient (Chatterjee, 2020) is relatively new metric for evaluating the rank correlation. Compared to traditional rank coefficients like Spearman corr., this coefficient is more effective to compute. It first rearrange the data as $\left[r^*(Y_{(1)}), r(Y_{(1)}\right], ..., \left[r^*(Y_{(N)}), r(Y_{(N)})\right]$ such that $r^*(Y_{(1)} \leq r^*(Y_{(2)} \leq ... \leq r^*(Y_{(N)})$, and then compute:

$$\xi_N \left(R(Y), R^*(Y)\right) = 1 - \frac{3 \sum_{i=1}^{N} |R_{(i+1)} - R_{(i)}|}{N^2 - 1} \tag{16}$$

8.9 The Relationship between Accuracy and Regret

Based on the assumption that only Regressional Goodhart takes effect and golden reward score $r^* \sim \mathcal{N}(0, \sigma_r^2)$, the noise $z \sim \mathcal{N}(0, \sigma^2)$, we can then derive the relationship between the accuracy and the regret. Based on the Regression Goodhart's, the proxy reward r can represented as:

$$r = r^* + z \tag{17}$$

The process of constructing an RM test set can be viewed as performing two independent samples from the distribution of the golden reward score. Therefore, the scores obtained from the two samples can be represented as $r_1 \sim \mathcal{N}(0, \sigma_r^2)$ and $r_2 \sim \mathcal{N}(0, \sigma_r^2)$. Subsequently, the difference between the two samples' golden reward scores also follows a normal distribution: $r_-^* \sim \mathcal{N}(0, 2\sigma_r^2)$. Then the proxy reward model score difference can be written as:

$$r_- = r_-^* - z_1 + z_2 \tag{18}$$

where z_1 and z_2 is the noise introduced in the two times of sampling. The distribution of noise difference is also normal distribution $z_1 - z_2 \sim \mathcal{N}(0, 2\sigma^2)$. The accuracy can be translated into:

$$\begin{aligned} d_r^{acc} &= P(r_- > 0, r_-^* > 0) + P(r_- < 0, r_-^* < 0) \\ &= P(r_- > 0, r_-^* > 0) \\ &= 1 - 2P(z_1 - z_2 < 0, r_-^* > 0) \\ &= 1 - 2 \int_{x=0}^{+\infty} P(x = r_-^*) P(z_1 - z_2 < x) dx \\ &= 1 - \int_{x=0}^{+\infty} \frac{1}{\sigma_r \sqrt{\pi}} e^{-\frac{x^2}{4\sigma_r^2}} \Phi\left(-\frac{x}{\sqrt{2}\sigma}\right) dx \end{aligned} \tag{19}$$

Following the notations in Section 2, we define the degree of overoptimization d_π as follows:

$$d_\pi = \frac{J_{r^*}(\pi)}{J_r(\pi)} \tag{20}$$

[3]One may expect this metric to compute the proxy rank of the response that receives the highest golden reward score. But our implementation makes it more similar to the Bo5 metric.

Table 8: Summary of Training Hyperparameters

RM Training Hyperparameters	Value	PPO Training Hyperparameters	Value
Max Length	2048	Train Batch Size	64
Regularization Coefficient	1e-2	Rollout Batch Size	8
Batch Size	256	Generate Max Length	1024
Warmup Ratio	0.1	Actor Learning Rate	1e-6
Learning Rate Scheduler	cosine	Critic Learning Rate	1e-5
Learning Rate	5e-6	KL Penalty	0

This value implies that if the expected reward of a policy π under the proxy RM is $\mathbb{E}(r) = c$, then the corresponding expected reward under the golden RM should be $mathbbE(r^*) = d_\pi c$. We then introduce a result from (Gao et al., 2022):

$$\mathbb{E}\left[X|X+Z=c\right] = \mathbb{E}[X] + (c - \mathbb{E}[X] - \mathbb{E}[Z])\frac{\text{Var}(X)}{\text{Var}(X)+\text{Var}(Z)} \tag{21}$$

where X and Z are independent, absolutely continuous random variables, both normally distributed. In our context, X can be replaced by r^* and $X+Z$ by r. Therefore, the degree of overoptimization d_π can be expressed as:

$$\begin{aligned} d_\pi &= \frac{\mathbb{E}_{y\sim\pi(\cdot|x)}[r^*(x,y)]}{\mathbb{E}_{y\sim\pi(\cdot|x)}[r(x,y)]} \\ &= \frac{\int_{-\infty}^{+\infty}\int_{-\infty}^{+\infty} r^* p(r^*,r)dr^*dr}{\int_{-\infty}^{+\infty} rp(r)dr} \\ &= \frac{\int_{-\infty}^{+\infty}\left[\int_{-\infty}^{+\infty} r^* p(r^*|r)dr^*\right]p(r)dr}{\int_{-\infty}^{+\infty} rp(r)dr} \\ &= \frac{\int_{-\infty}^{+\infty}\frac{r\sigma_r^2}{\sigma_r^2+\sigma^2}p(r)dr}{\int_{-\infty}^{+\infty} rp(r)dr} \\ &= \frac{\sigma_r^2}{\sigma_r^2+\sigma^2} \end{aligned} \tag{22}$$

Under the BoN setting, we first normalize the reward scores and directly estimate d_π according to the definition in equation 20.

8.10 Details about Experiments

For all experiments in Section 4, we obtain the results through multiple samplings of test datasets. Specifically, in Figure 4, we perform 64 samplings for each chosen-reject rank bin to construct different test datasets and calculate their correlation with downstream performance. The final results are averages of these outcomes. For Tables 2, 3, and 4, the set of prompts is fixed, but we sample multiple different responses for each prompt, conducting 64 samplings to construct various test datasets. These outcomes are used to calculate the mean and variance for reporting correlations. In Figures 5, 6, and 7, neither the test prompts nor responses are fixed. For each data point, we perform 64 samplings to obtain different test datasets and calculate the results, which are reported with the 95% confidence interval.‘1 Next, we provide training details. The hyperparameters for RM and PPO training are listed in Table 8. For PPO optimization, we utilize the OpenRLHF framework (Hu et al., 2024). In BoN optimization, N is set to 1280, requiring $2733 \times 1280 \times 10 = 34,982,400$ response samplings and RM scoring for preparing BoN results. In the KL divergence calculation for BoN, we use a logarithm base of 2.